Astronomy & Astrophysics

Millimetric observations of southern H II regions

L. Sabbatini[1], F. Cavaliere[2], G. Dall'Oglio[1], R. D. Davies[3], L. Martinis[1], A. Miriametro[4],
R. Paladini[5], L. Pizzo[1], P. A. Russo[1], and L. Valenziano[6]

[1] Dipartimento di Fisica, Università di Roma Tre, via della Vasca Navale 84, 00146 Roma, Italy
  e-mail: sabbatini@fis.uniroma3.it
[2] Dipartimento di Fisica, Università di Milano, via Celoria 16, 20133 Milano, Italy
[3] University of Manchester, Jodrell Bank Observatory, Macclesfield, Cheshire, UK
[4] Dipartimento di Fisica, Università di Roma "La Sapienza", Roma, Italy
[5] CESR, 9 Avenue du Colonel Roche, BP 4346, 31028 Toulouse Cedex 4, France
[6] CNR, IASF, sezione di Bologna, via P. Gobetti 101, 40129 Bologna, Italy

Abstract. We report on millimetric continuum observations of two bright compact H II regions, which have been observed for the first time in this frequency range. For the two observed regions (G291.6-0.5 and G291.3-0.7), we derive the flux densities at the two observed wavelengths (1.25 and 2 mm) as well as the spectral index and the temperature of the surrounding dust by fitting a modified blackbody curve to our results combined with IR values obtained from the literature. We also estimate the dust mass and the bolometric luminosity of the two regions.

Key words. H II regions – ISM: individual objects: G291.6-0.5 – ISM: individual objects: G291.3-0.7 – submillimeter – dust, extinction

1. Introduction

H II regions are among the brightest sources in the Galaxy. They represent the final stages of the birth of young, massive stars of O and B spectral types. When reaching the Zero Age Main Sequence, the young massive star is still deeply embedded in a dense gas and dust nebula; the star heats the dust and ionizes the hydrogen in the surrounding envelope. Radio observations of these sources are dominated by free-free emission originated in the ionized nebula; the infrared part of the spectrum, instead, is due to dust emission and can be described by a modified blackbody curve. While many radio and IR observations of these objects are available, only few of them have been observed in the millimeter range up to now.

There are many interesting, still unsolved problems related to the physical properties of the ionized region and its surrounding dust cocoon. Because the heating mechanisms are different and because the two components may be differently distributed within a source, the free-free and the dust emission do not have to be spatially coincident. A displacement between the radio and the FIR contours of emission in M17 has indeed been detected (Wilson et al. 1979; Gatley et al. 1979). However, more information is required to confirm this result.

In addition, this work has been motivated by the role played by H II regions in the context of Cosmic Microwave Background (CMB) measurements.

Since H II regions are non-variable, bright, compact sources, they represent viable candidates for calibration and pointing/beamshape reconstruction in case of CMB imaging experiments such as the space-borne mission PLANCK by ESA[1] scheduled for launch in 2007.

We selected a sample of southern compact H II regions, using the Paladini et al. radio catalog (2003) and adopting the following selection criteria: i) the source elevation is required to be greater than 30° to assure good conditions of observation; ii) the extrapolated flux density from radio observations, due to free-free emission, is chosen to be greater than about 10 Jy at millimeter wavelength; iii) the angular dimension of the source should match the characteristics of the telescope (a few arcmin). The application of these criteria has produced a list of 12 sources, which have been observed during the XVII Italian Antarctic Expedition. Our observations provide for these sources complementary information to the existing radio and infrared data, therefore allowing the reconstruction of the spectral behavior across a wide frequency range and the joint analysis of free-free and thermal dust emission. Generally, the lack of millimetric observations is mainly due to limitations introduced by atmospheric absorption. Among the atmospheric constituents, the strongest millimetric absorber is water vapor; high and/or dry places, such as Antarctica, are required in order to achieve a low content of water vapor, corresponding to a

---

[1] http://esa.nl

high level of transmission. In this paper, we report our results for two of the observed regions, G291.6-0.5 and G291.3-0.7.

2. The observing site

Antarctica is considered the best site on Earth for millimetric and sub-millimetric observations, because of clean and steady air, low water vapor content, little interference of human activities. Observations reported in this paper were made from a sea-level site, Terra Nova Bay (Lat. 74°41′42″S, Long. 164°07′23″E), where the Italian station is operating from October to February, during the antarctic summer. During this period, lowest Precipitable Water Vapor (PWV) values are reported in the first two months, when the ice pack is still frozen. Moreover, when cold, dry winds from the inner continent are blowing, transparency may be exceptionally good. Although not as good as on the high Plateau, atmospheric conditions are comparable to a midlatitude observatory, such as those on the European Alps (see e.g. Mannucci 2003) or on the Canary Islands (see e.g. Watson et al. 2003).

Typical values measured using radiosoundings are reported in Fig. 1 (courtesy by ENEA); data refer to summer 1994 and 1995, when the site was fully characterized. The content of water vapor was monitored also during the period of the observations, using data kindly provided by ENEA. The PWV, as determined from radiosounding twice a day (see Fig. 2), was found being between 2.6 and 3 mm, corresponding to an atmospheric transmission of about 80% for the 1.25 mm channel and 90% for the 2 mm one, a typical value for Antarctic summer at sea level.

3. Equipment and observing strategy

The observations were carried out in the period from October to December 2001, from the O.A.S.I. telescope (Infrared and Submillimetric Antarctic Observatory). The telescope has a Cassegrain configuration, with a 2.6 m primary mirror, supported on an altitude-azimuth mount; the tracking accuracy is 30 arcsec. For more details on the telescope we refer to Dall'Oglio et al. (1992).

The detector is a bolometric system cooled at 0.3 K with a ^{3}He refrigerator operating at $\lambda_1 = 1.25$ mm and $\lambda_2 = 2$ mm of wavelength (corresponding to frequencies $\nu_1 = 240$ GHz and $\nu_2 = 150$ GHz respectively). The mesh filters used for the observations define the spectral bandwidths of $\Delta\nu_1 = 70$ GHz and $\Delta\nu_2 = 40$ GHz for the two channels, suitable to match the atmospheric windows. In this configuration, the *FWHM* beamwidth, as measured using bright sources, is θ_{FWHM} 5.9 arcmin. The detector output is acquired as a voltage V across the bolometer.

In order to remove the atmospheric contribution we adopted an ON-OFF technique, spending 15 min tracking the source (ON) and 15 min tracking the blank sky (OFF); the signal acquired on-source V_{ON} is due to both source and atmosphere, while the signal acquired off-source V_{OFF} is due only to the atmosphere. The source peak flux density is obtained by subtracting V_{OFF} to V_{ON}.

Moreover, we adopted a modulating secondary mirror to achieve a beam-switching and subtract any linear gradient of
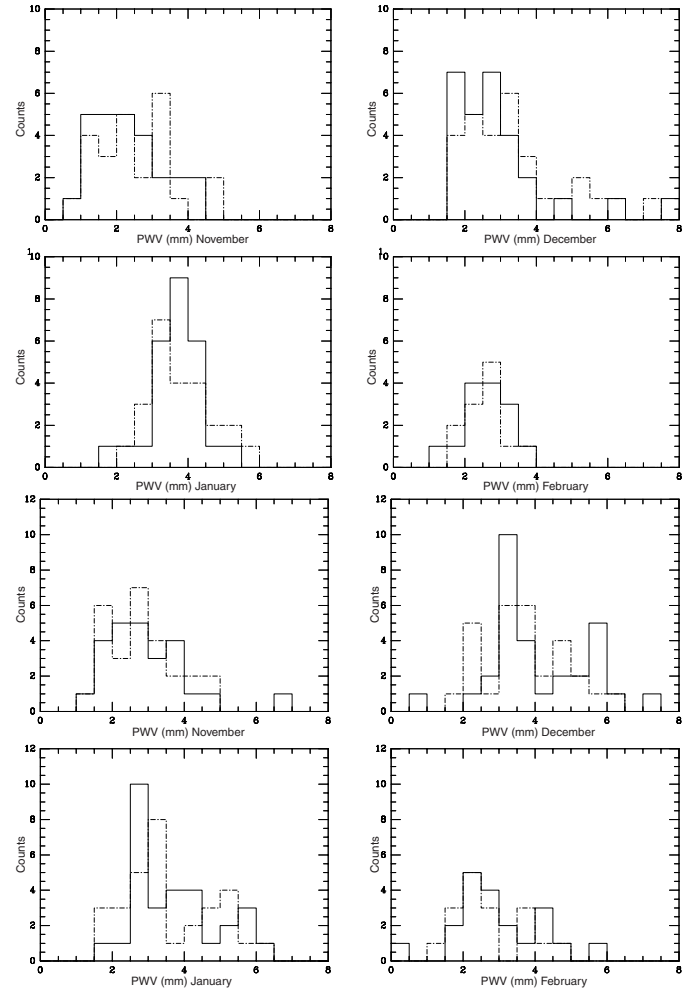

Fig. 1. PWV measured from radiosoundings in 1994 (*top panel*) and 1995 (*bottom panel*) at Terra Nova Bay during the summer (courtesy by ENEA). Typical values are around 3 mm; continuous line refer to 13.00 Local Time data, dot-dashed line to 01.00 LT.

temperature; in this three-fields modulation, the source is kept in the central field. The modulation is sinusoidal, with an amplitude of 18 arcmin and a frequency $\nu_{mod} \simeq 5.3$ Hz. The modulation frequency is chosen in a range where the bolometers have an optimal frequency response and are not affected by the 1/f noise; the modulation is always parallel to the horizon. The signal due to the central field, which has a frequency of two times the modulation frequency ν_{mod}, is demodulated by a lock-in amplifier. The lock-in amplifier is also used to integrate the detector signal for 3 s to remove high frequency fluctuations. Both the detector signal and the output of the lock-in amplifier for the two channels were collected by a data acquisition system, which sampled the output 64 times per second. For flux density calibration we used Venus, adopting a temperature of 276 K for the first channel ($\lambda_1 = 1.25$ mm, Werner & Neugebauer 1978) and 294 K for the second one ($\lambda_2 = 2$ mm, Ulich 1981), with an error of about 7%.
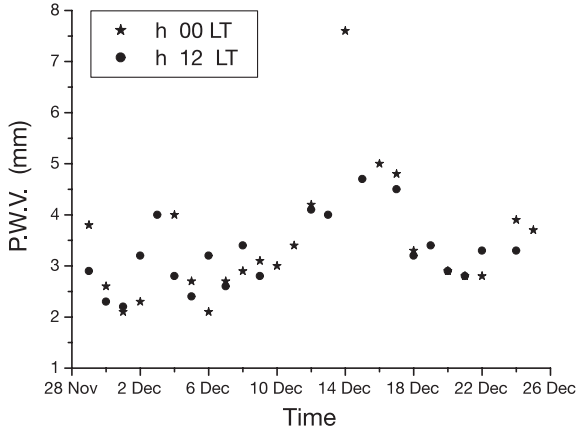
Fig. 2. PWV obtained from calculations on radiosoundings in the period of observations (October–December 2001).

4. Analysis of observations

We have used a polynomial fit to remove the baseline variations due, for instance, to slow variation of detectors temperature. We have chosen a polynomial function on the basis of a chi-square test: we found that a parabolic fit well reproduces the fluctuations on time scales of order of 30 min. The removal of the baseline significantly reduces the signal fluctuations which decrease from 20% to 12%. After removing the baseline, we have computed the difference $V_i = V_i^{ON} - V_i^{OFF}$ for each ON-OFF cycle; our best estimate for the peak flux density of the source is determined as the mean $\sum_{i=1}^{N} \frac{V_i}{N}$, multiplied by the corresponding calibration coefficient.

The peak flux density is then corrected for atmospheric attenuation, since Venus is at a much lower elevation than the observed H II regions; we take into account the different airmasses by multiplying the peak flux density for a factor that accounts for atmospheric transmission at different elevation.

In order to convert the corrected peak flux density S_{peak} to an integrated one it is essential to know the intrinsic size of the source. Information about the size has been obtained using radio and FIR maps in the following way: an elliptical shape is superimposed on the central part of the map of the two considered H II regions both in radio and FIR range. Profiles of the source emission have been extracted along major and minor axes of the ellipse; then, a Gaussian function has been superimposed on each of those profiles, allowing the evaluation of the dimensions θ_G.

Radio values have been convolved with our telescope beamwidht θ_{beam} of 5 arcmin (related to the *FWHM* of 5.9 arcmin by the relation $\theta_{FWHM} = \theta_{beam} \sqrt{2 \times \ln 2}$) using the formula $\theta_{source} = \sqrt{\theta_G^2 + \theta_{beam}^2}$. Far infrared data have been evaluated on maps already smoothed at 5 arcmin, hence the deconvolution has not been applied.

Table 1 reports the angular diameters obtained from the literature for the two sources observed. It is worth noting that for each source the values of the diameters found in the radio are comparable to the IR ones. Since the radio emission is due to the ionized hydrogen and the FIR one is coming from the dust envelope, the similarity between the sizes at various

frequencies suggests that the two components of the nebula are coupled. This aspect could be proved by observations at higher angular resolution. If we consider the two components (ionized gas and dust) as bound, it is straightforward to associate at millimeter wavelengths a dimension that is between the ones measured in the radio and the ones from the infrared. Hence, values reported for this work are the result of an extrapolation between radio and infrared observations. Those values suffer the uncertainties due to the extrapolation and uncertainties in the original radio and infrared maps.

We note that the angular dimensions of G291.3-0.7 are smaller than the *FWHM* beamwidth of 5.9 arcmin, hence the flux is completely collected by the receiver and no correction is required to convert the peak flux density. The source G291.6-0.5, on the contrary, is more extended than the beamwidth, thus we have to derive an integrated flux density S_{tot} from the observed peak flux S_{peak} assuming a Gaussian profile and using $S_{tot} \propto S_{peak} \theta_1 \times \theta_2$, where θ_1 and θ_2 are the beamsmoothed widths of the source along its main axes.

Table 1 also reports our results for the integrated flux density for the two observed H II regions, together with radio and FIR data taken from the literature.

Uncertainties in our results can be attributed to both errors in calibration and fluctuations in the source observation. For what concerns the calibration, we should evaluate: i) the uncertainty on the expected flux of Venus ($\sigma_{Venus} = 7\%$); ii) the signal fluctuation on the measure (negligible for calibration, due to the high S/N value); iii) the error on the evaluation of the atmospheric transmission (σ_{atmo}).

For the source observation, we have to consider the fluctuations of the signal ($\sigma_{source} = 12\%$ after the baseline removal) and again the error on the evaluation of the atmospheric transmission (σ_{atmo}). The error on the transmission is evaluated using values of the PWV for the period of observations and a model for atmospheric attenuation; we found $\sigma_{atmo}(1.25 \text{ mm}) = 5.5\%$ for the 1.25 mm channel and $\sigma_{atmo}(2 \text{ mm}) = 1.2\%$ for the 2 mm one, both for Venus and sources observations.

If we consider these quantities as uncorrelated, we can add them quadratically and get $\sigma_{tot} = \sqrt{\sigma_{Venus}^2 + \sigma_{source}^2 + 2\sigma_{atmo}^2}$. Finally, we find $\sigma_{tot}(1.25\text{mm}) = 16\%$ and $\sigma_{tot}(2\text{mm}) = 14\%$.

5. Results

In the following we report both the main properties of the two sources, as derived from the literature, and our results.

G291.6-0.5. Eastern part of RCW 57. Celestial coordinates at 2000: RA 11h 15m 08s, Dec –61°14'36''. The source has a large size and irregular shape (see Table 1). It is probably the most massive optically visible H II region in the Galaxy (Goss & Radhakrishnan 1969). The published solar distance varies between 7.0 (Moffat 1983) and 8.6 kpc (Caswell & Haynes 1987). Assuming that this source is 8.2 kpc from the Sun, it is one of the most powerful thermal radio sources of the Galaxy (Wilson et al. 1970, see Table 1). Wilson et al. also derive some physical parameters, including emission measure ($E = 7.5 \times 10^5$ cm^{-6} pc), mass of

Table 1. Data about the two observed H II regions. For each source, values for angular dimensions (arcmin) and flux density (Jy) are reported at various frequencies, with the relative reference.

		G291.6-0.5		G291.3-0.7		
ν(GHz)	λ	$\theta_1 \times \theta_2$	S_ν	$\theta_1 \times \theta_2$	S_ν	Reference
0.408	73 cm	9.4×7.1	180	3.5×3.0	23	Shaver & Goss (1970)
2.7	11 cm	9.2×8.0	238	5.0×5.0	95	Thomas & Day (1969)
5.0	6 cm	8.6×7.1	178	0.9×0.9	95	Caswell & Haynes (1987)
5.0	6 cm	8.5×6.4	–	3.9×3.9	–	Goss & Shaver (1970)
150	2 mm	10.0×6.5	208	4.0×4.0	68	This work
240	1.25 mm	10.0×6.5	367	4.0×4.0	97	This work
3.0×10^3	100 μm	11.6×7.1	68 900	4.9×4.7	21 000	Schlegel et al. (1998)
5.0×10^3	60 μm	9.8×6.9	75 000	3.9×3.9	13 000	Schlegel et al. (1998)
1.2×10^4	25 μm	7.8×6.1	29 400	4.3×3.3	4290	Schlegel et al. (1998)
2.5×10^4	12 μm	7.5×5.8	5200	4.3×3.5	659	Schlegel et al. (1998)

ionized hydrogen ($M_{\mathrm{H\,II}} = 1.3 \times 10^4\ M_\odot$) and electron density ($N_\mathrm{e} = 208\ \mathrm{cm}^{-3}$).

G291.3-0.7. Western most component of RCW 57. Celestial coordinates at 2000: RA 11h 12m 11s, Dec –61°19′07″. It has a small angular size (cf. Table 1). Its kinematic distance is estimated in 3.6 kpc (Wilson et al. 1970; Caswell & Haynes 1987). This value is also supported by OH and H I absorption lines (Goss & Radhakrishnan 1969). Calculations by Wilson et al. (1970) retrieve the following values for the physical parameters: emission measure ($E = 1.4 \times 10^7\ \mathrm{cm}^{-6}\,\mathrm{pc}$), mass of ionized hydrogen ($M_{\mathrm{H\,II}} = 9.9 \times 10^1\ M_\odot$) and electron density ($N_\mathrm{e} = 3122\ \mathrm{cm}^{-3}$).

The distance between the two sources along the line of sight is about 5 kpc.

Figure 3 shows the spectrum of the two H II regions. At frequencies lower than the so-called *turnover* frequency ν_0 (around a few GHz), the cloud is optically thick and the flux is partially self-absorbed from the cloud itself. For frequencies between a few GHz to about one hundred GHz the spectrum shows the feature of the free-free emission, with a power-law of the form $\nu^{-0.15}$ (Mezger & Henderson 1967). At higher frequencies ($\nu \geq 100$ GHz) the spectrum is dominated by dust emission. In the case of G291.3-0.7 the turnover frequency is ~3 GHz as expected for its high emission measure of $1.4 \times 10^7\ \mathrm{cm}^{-6}\,\mathrm{pc}$. For G291.6-0.5 the turnover is $\lesssim 1$ GHz as implied by its lower value of E.

Our measurements, combined with IRAS data taken from the literature, allow the determination of the physical properties of the dust of the two observed sources. By fitting a modified Planck curve – for which we adopt the notation of Chini et al. 1986a, $\nu^m B_\nu(T_\mathrm{d})$ – to the observations at FIR and millimetric wavelengths, we obtain an estimate of the spectral index m and the dust temperature T_d.

As expected, it is not possible to describe the whole set of data, from 2000 μm to 12 μm with a single curve. In fact, while the long-wavelength part of the spectrum accounts for the emission from relatively cool dust far from the central source, the excess at mid-infrared wavelengths is due to a small amount of dust at a much higher temperature, in the proximity of the star/cluster of stars. Thus, only the IRAS 100 μm flux, together with our results at 1.25 and 2 mm, were used in the fitting analysis. Values for the flux density were corrected by
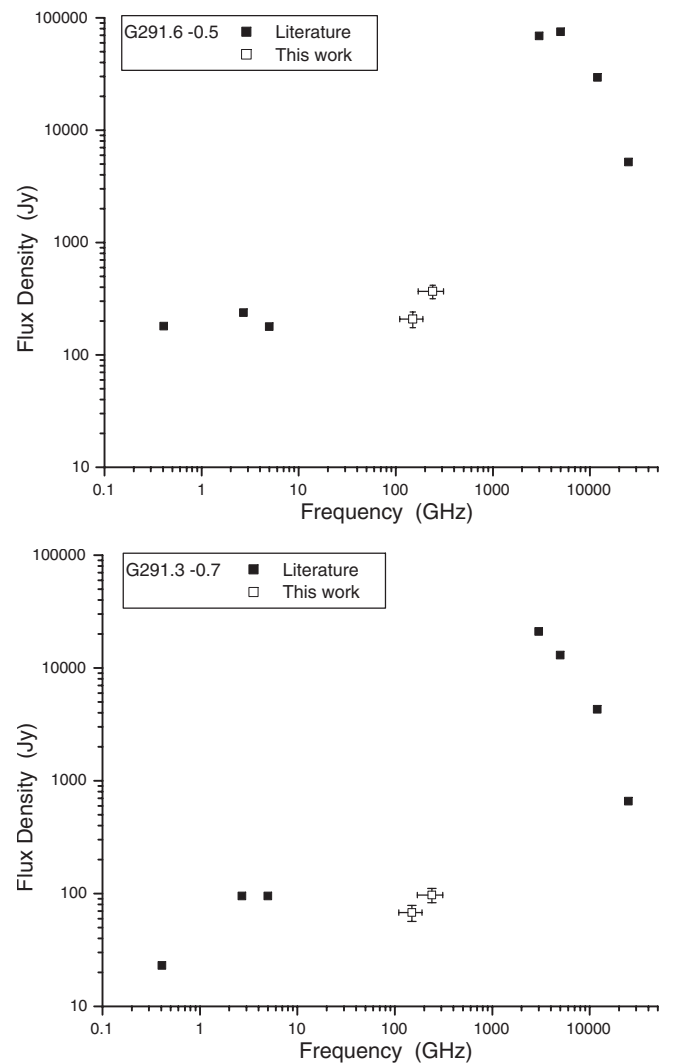

Fig. 3. Spectra of the two observed H II regions: G291.6-0.5 (*top*) and G291.3-0.7 (*bottom*). Our results are reported with an open square, with the corresponding error bars, while data from the literature (see Table 1) are reported with a filled square.

subtracting the free-free contribution, in order to account only for the dust content. The free-free contribution was evaluated

Table 2. Results for spectral index m and dust temperature T_d, with the corresponding statistical uncertainties.

Source	m	T_d (K)
G291.6-0.5	1.58 ± 0.01	25.6 ± 0.7
G291.3-0.7	1.50 ± 0.01	31.3 ± 0.7

by extrapolating radio fluxes with a power-law of the form $\nu^{-0.15}$. Our results for m and T_d are summarized in Table 2.

The values found for temperature ($25 \div 31$ K) are comparable with those reported in the literature (see Chini et al. 1986a,b; Mueller et al. 2002). By comparison, Chini et al. (1986a,b) find for example an average temperature of 26 K, for a spectral index $m = 2$. Their work, although covering a large sample of H II regions (57 sources), is limited by the use of a single observed value of flux density at millimeter wavelengths ($\lambda = 1.3$ mm). This implies that, in order to fit only two experimental points (at 1.3 mm and 100 μm) with a modified blackbody function, one of the two parameters of the function (m and T_d) has to be fixed a priori. In our work, having three experimental points for each source, we don't need to make any assumption for the value of m. Therefore, both parameters are found analytically.

Our results for flux densities and for dust temperature may be used to infer some physical parameters of the two sources, such as their dust masses and bolometric luminosities. In the following, for angular dimensions and distances we adopt the values given by Caswell & Haynes (1987), because their observations have the highest spatial resolution among the radio data (with the exception of the 0.408 GHz observations of Shaver & Goss 1970, that have not been used because they lie in the self-absorption part of the spectrum). Hence, hereafter we adopt for G291.6-0.5 a distance of 8.6 kpc and angular dimensions of $7' \times 5'$, while for G291.3-0.7 the distance is 3.6 kpc and the angular dimensions are $0.9' \times 0.9'$.

Assuming that the dust cloud is optically thin, its mass can be estimated using the formula $M_d = \frac{F_\nu D^2}{k_\nu B_\nu(T_d)}$ where F_ν is the flux density due to dust emission (hence the total flux reduced by the bremsstrahlung contribution), D is the distance of the source from the Sun, $B_\nu(T_d)$ is the blackbody function at temperature T_d and k_ν is the dust mass absorption coefficient, $k_\nu = 0.9$ cm^2 g^{-1} at $\lambda = 1.3$ mm (Ossenkopf & Henning 1994). The dust masses, obtained using our observations at 1.25 mm and our estimate for T_d, are about 3×10^3 $M_\odot$ for G291.6-0.5 and 70 $M_\odot$ for G291.3-0.7.

For each source, the bolometric luminosity L_{bol} is calculated by integrating the spectral energy distribution over the frequencies, interpolating the data from the radio to the infrared (including our new millimeter results). The values obtained for L_{bol} for the two sources are 1.85×10^7 $L_\odot$ for G291.6-0.5 and 4.24×10^5 $L_\odot$ for G291.3-0.7.

Finally, it is also possible to estimate the likely star mix responsible for the H II region. For this purpose, it is mandatory to know the intrinsic size of the two sources. According to Caswell & Haynes (1987), G291.6-0.5 has an angular extent of $7' \times 5'$ at a distance of 8.6 kpc, hence its diameter (computed as the geometric mean) is of 14.8 pc; for G291.3-0.7, assuming

an angular diameter of $0.9' \times 0.9'$ and a distance of 3.6 kpc, the diameter is of about 0.94 pc. Using these values and the electronic densities as given by Wilson et al. (1970) (208 and 3122 cm^{-3} respectively), we compute the excitation parameter $U = r\, n_e^{2/3}$, that is about 260 and 100 pc cm^{-2} (slightly lower than those reported by Wilson et al. (1970), of 304 and 147 pc cm^{-2}, due to differences in the estimate of distances and diameters). Finally, we compute the Lyman continuum photon flux needed to maintain the ionization of the nebula using the relation $N_c \geq 8.04 \times 10^{46} T_e^{-0.85} U^3$ (Kurtz et al. 1994), where T_e is the electron temperature as reported by Wilson et al. (1970) (6900 K and 7700 K). We found that N_c is 7.69×10^{50} s^{-1} for G291.6-0.5 and 4.17×10^{49} s^{-1} for G291.3-0.7. Assuming that the central stars are of spectral type O5 V (corresponding to a luminosity of about 4.9×10^{49} s^{-1}, see Panagia 1973), we found that the G291.6-0.5 region is excited by a cluster of 16 stars, while a single star could provide the photon flux needed to ionize the G291.3-0.7 region.

6. Conclusions

We have presented the first observations at 1.25 and 2 mm of two compact H II regions, G291.6-0.5 and G291.3-0.7. For these sources, by combining our measurements with IRAS ones, we have derived the spectral index and the temperature of the dust.

We find an average $m = 1.54$ and temperature $T_d \sim 28$ K. The wavelength dependence of the emissivity of the emitting dust grains contains information on their nature: $m = 2$ implies crystalline grains (Aannestad 1975) whereas $m = 1$ suggests an amorphous structure (Koike et al. 1980). Our result seems to slightly favor a crystalline structure.

We estimate the dust mass and the bolometric luminosities of the two nebula; the likely star mix responsible for the H II regions is also determined.

By comparing radio and FIR data from the literature for the two H II regions, we find that the angular dimensions of the ionized region and the dust nebula are very similar. This could suggest that, indeed, the two components of emission are tightly coupled and deeply interacting. Clearly, further observations of H II regions at far-infrared and submillimetric wavelength are required in order to confirm the nature of the emitting grains in star-forming regions as well as the presence of other components of emission at different temperatures and the interactions between the ionized gas and the dust.

References

Aannestad, P. A. 1975, ApJ, 200, 30
Caswell, J. L., & Haynes, R. F. 1987, A&A, 171, 261
Chini, R., Kreysa, E., Mezger, P. G., & Gemund, H. P. 1986, A&A, 154, L8

Chini, R., Kreysa, E., Mezger, P. G., & Gemund, H. P. 1986, A&A, 157, L1

Dall'Oglio, G., Ade, P. A. R., Andreani, P., et al. 1992, ExA, 2, 275

Gatley, I., Becklin, E. E., Sellgren, K., & Werner, M. W. 1979, ApJ, 233, 575

Gear, W. K., Robson, E. I., & Griffin, M. J. 1988, MNRAS, 231, 55

Gordon, M. A. 1987, ApJ, 316, 258

Goss, W. M., & Radhakrishnan, V. 1969, Astrophys. Lett., 4, 199

Goss, W. M., & Shaver, P. A. 1970, AuJPA, 14, 1

Koike, C., Hasegawa, H., & Manabe, A. 1980, Astrophys. Space Sci., 67, 495

Kurtz, S., Churchwell, E., & Wood, D. O. S. 1994, ApJS, 91, 659

Mannucci, F. 2003, Mem. Soc. Astron. It., 74, 101

Mezger, P. G., & Henderson, A. P. 1967, ApJ, 147, 471

Moffat, A. F. J. 1983, A&A, 124, 273

Mueller, K. E., Shirley, Y. L., Evans N. J., & Jacobson, H. R. 2002, ApJS, 143, 469

Ossenkopf, V., & Henning, Th. 1994, A&A, 291, 943

Paladini, R., Burigana, C., Davies, R. D., et al. 2003, A&A, 397, 213

Panagia, N. 1973, AJ, 78, 929

Shaver, P. A., & Goss, W. M. 1970, AuJPA, 14, 77

Schlegel, D. J., Finkbeiner, D. P., & Davis, M. 1998, ApJ, 500, 525

Thomas, B. M., & Day, G. A. 1969, AuJPA, 11, 3

Ulich, B. L. 1981, AJ, 86, 1619

Watson, R. A., Carreira, P., Cleary, K., et al. 2003, MNRAS, 341, 1057

Werner, M. W., & Neugebauer, G. 1978, Icarus, 35, 289

Wilson, T. L., Mezger, P. G., Gardner, F. F., & Milne, D. K. 1970, A&A, 6, 364

Wilson, T. L., Fazio, G. G., Jaffe, D., et al. 1979, A&A, 76, 86